Elastic Scattering of 146-Mev Polarized Protons by Deuterons*

HERMAN POSTMA† AND RICHARD WILSON
Cyclotron Laboratory, Harvard University, Cambridge, Massachusetts
(Received October 7, 1960)

The polarization and differential cross section of 146-Mev protons elastically scattered by deuterons have been measured in the center-of-mass angular range from 3.9° to 170°. A description of the liquid deuterium target and detection apparatus which permitted the measurement of the elastic events over these angles is given. At small angles the proton was energy analyzed; at large angles the recoil partner of the proton, the deuteron, was identified and energy analyzed. Although the energy resolution of ±1.7 Mev and the angular resolution of ±2.0° were sufficient to separate quasi-elastic events from elastic events at most angles, they were insufficient to resolve unambiguously the 2.3-Mev inelastic events resulting from the formation of virtual deuterons. The measured cross section is in qualitative agreement with cross sections at neighboring energies; no comparison of measured polarizations is possible due to the lack of other experiments. The cross sections and polarization for angles less than 80° c.m. are well fitted by the Kerman, McManus, and Thaler theory using the Gammel and Thaler nucleon-nucleon potential description. The energy and angular dependence of the large-angle pickup cross section proposed by Chew and Goldberger agree well with experiment; however, the small measured positive polarization is not predicted by this theory, and probably indicates destructive interference between the direct and the pickup scattering.

INTRODUCTION

THE role of polarized nucleon-deuteron scattering in an attempt to learn more about nuclear forces is manifold. Although the nucleon-deuteron interaction is a three-body problem, theoretical apparatus in the form of the impulse approximation is able to relate this interaction to a superposition of nucleon-nucleon interactions. Since phase shifts from nucleon-nucleon scattering experiments at this energy are not yet available, the phase shifts calculated from assumed nucleon-nucleon potentials must be used in this superposition.[1] A comparison between the experimental data and theoretical prediction in the small center-of-mass angular region in which direct elastic scattering takes place gives information on how meaningful the combination of nucleon-nucleon potential and superposition approximation is. At the large center-of-mass angles where "deuteron pickup"[2] dominates we can learn more about the high momentum components in the deuteron, the deuteron wave function, and the nature of the interference between the direct and pickup processes. "Quasi-elastic" scattering[3] by the nucleons in the loosely bound deuteron can be compared directly to their free scattering counterparts by again using the impulse approximation. Scattering resulting in the formation of the virtual singlet state of the deuteron gives further information about the superposition of nucleon-nucleon scattering amplitudes. Finally, since targets of neutrons do not exist, neutron-deuteron scattering is the closest approach to *n-n* scattering; a comparison of *n-d* and *p-d* scattering can answer the question of whether or not nuclear forces are charge symmetric.

The largest number of nucleon-deuteron experiments at higher energies has been confined to measurements of the elastic differential cross section. Proton-deuteron scattering has been studied by Caldwell[4] (20.6 Mev *p-d*); Ashby[5] (32 Mev *p-d*); Chamberlain and Stern[6] (192 Mev *d-p*); Cassels, Stafford, and Pickavance[7] (145 Mev *p-d*); Schamberger[8] (240 Mev *p-d*); Chamberlain and Clark[9] (340 Mev *p-d*); and Crewe[10] (450 Mev *p-d*). Neutron-deuteron scattering has been studied by Powell[11] (90 Mev *n-d*); and Youtz[12] (90 Mev *n-d*). The pickup region has been studied by Bratenahl[13] (95, 112, 138 Mev *p-d*) and Teem[14] (95 Mev *p-d*). Polarization alone has been investigated at three angles by Marshall, Marshall, Nagle, and Skolnik[15] (310 Mev *p-d*). None of these experiments were extended into the small-angle Coulomb interference region. The present experiment includes both polarization and differential cross section for most of center-of-mass angular range. It is particularly valuable now because of the appearance of *p-p* and *n-p* double and triple scattering experiments being

* Supported by the joint program of the Office of Naval Research and the U. S. Atomic Energy Commission.
† Now at Oak Ridge National Laboratory, Oak Ridge, Tennessee.
[1] A. K. Kerman, H. McManus, and R. M. Thaler, Ann. Phys. **8**, 551 (1959), Nucl. Phys. **10**, 151 (1959). Similar calculations are also made by J. Sawicki and S. Watanabe and by L. Castillejo and L. S. Singh, *Nuclear Forces and the Few-Nucleon Problem* (Pergamon Press, New York, 1960), p. 193.
[2] G. F. Chew and M. L. Goldberger, Phys. Rev. **77**, 470 (1950).
[3] G. F. Chew, Phys. Rev. **80**, 196 (1950); G. F. Chew, Phys. Rev. **84**, 710 (1951); G. F. Chew, Phys. Rev. **84**, 1057 (1951).
[4] D. Caldwell, J. R. Richardson, and H. N. Royden, Bull. Am. Phys. Soc. **28**, 7 (1953).
[5] V. J. Ashby, University of California Radiation Laboratory Report UCRL-2091 (unpublished).
[6] O. Chamberlain and M. O. Stern, Phys. Rev. **94**, 666 (1954).
[7] J. M. Cassels, G. H. Stafford, and T. G. Pickavance, Nature **168**, 556 (1951).
[8] R. D. Schamberger, Phys. Rev. **85**, 424 (1952).
[9] O. Chamberlain and D. D. Clark, Phys. Rev. **102**, 473 (1956).
[10] A. V. Crewe, B. Ledley, E. Lillethun, S. Marcowitz, and L. G. Pondrom, Phys. Rev. **114**, 1361 (1959); S. Marcowitz, Phys. Rev. **120**, 891 (1960).
[11] W. Powell, University of California Radiation Laboratory Report UCRL-1191 (unpublished).
[12] B. L. Youtz, University of California Radiation Laboratory Report UCRL-2307 (unpublished).
[13] A. Bratenahl, University of California Radiation Laboratory Report UCRL-1842; A. Bratenahl, Phys. Rev. **92**, 538 (1953).
[14] J. M. Teem, Ph.D. thesis, Harvard University, 1954 (unpublished).
[15] L. Marshall, J. Marshall, D. Nagle, and W. Skolnik, Phys. Rev. **95**, 1020 (1954).

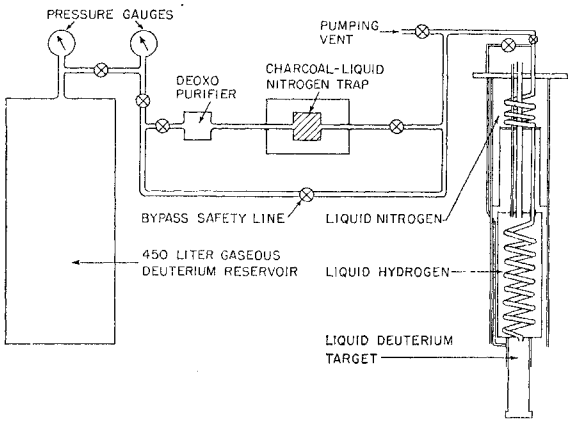

FIG. 1. Deuterium condensation system.

done at the same energy of 146 Mev.[16–20] A completion of these will permit the calculation of phase shifts directly from experimental data rather than from assumed potentials and thus will allow a direct comparison of the theory of superposition with proton scattering from the simplest of complex nuclei—the deuteron.

THE EXPERIMENT

The difference between the number of right and left events for an incident polarized proton beam appears quantitatively as the asymmetry e_d produced by the deuterons and bears the following relation to the polarizations[21]:

$$e_d = P_B P_d = (N_L - N_R)/(N_L + N_R), \qquad (1)$$

where P_B is the initial polarization of the proton beam and P_d is the polarization produced by the deuterons.

Averaging N_L and N_R gives the N_0 for an incident unpolarized beam[21] which appears in the cross section. To determine the differential cross section and polarization for p-d scattering it is necessary to measure the incident beam intensity, energy and degrees of polarization, N_R and L_L to areal density of target atoms, and solid angle. A cylindrical liquid deuterium target 1.83 in. in diameter and 3 in. high was constructed to avoid backgrounds that are present when the deuteron is in combination with another element. A schematic diagram of the target and condensation system is shown in Fig. 1. The target cup was made from two-mil thick Mylar sheet sealed into cylindrical form by thermal setting araldite.[22] A closed free-flow system permitted the reuse of the deuterium. From the 450-liter storage tank the gaseous deuterium, initially at one atmosphere of pressure, flowed through a filter network to the condensation target system. Here it was first cooled to 77°K in the coils in the liquid nitrogen bath and then condensed at 20.4°K in coils immersed in a liquid hydrogen reservoir. This condensation continued rapidly until the pressure of the liquid deuterium in the target chamber equaled the pressure in the storage tank (one-third atmosphere). This condensation-target assembly was surrounded by heat shields maintained at liquid nitrogen temperature and placed in a vacuum system. The purity of deuterium (99.7%), the vapor pressure at 20.4°K, and the target diameter (1.83 in.) led to an areal density of $(2.35\pm0.05)\times10^{23}$ deuteron-atoms/cm^2.

TABLE I. Elastic proton-deuteron kinematical results.

θ Center-of-mass angle	ϕ Deuteron lab angle	Proton lab angle	E_d Deuteron lab energy Mev	E_p Proton lab energy Mev
3.90	88.0	2.46		144
7.70	86.0	5.0		143
13.93	82.7	9.0		142
38.40	70.3	25.0		129
75.08	52.0	50.0	40	95
99.93	40.2	70.0	68	66
109.07	35.0	77.5	86.6	56
159.67	10.0	140.6	126.4	

The elastic particles that scatter from deuterium must be distinguished from the particles arising from other processes that are taking place. The proton must be distinguished from the deuterons, and then the identified particles energy analyzed to insure that they arose from elastic processes in the deuterium target.

A target thickness of several Mev together with the kinematical relations tabulated in Table I suggest immediately that several different detection schemes must be employed to cover the entire center-of-mass (c.m.) angular range. At small angles (4°–75° c.m.) the proton was measured because its recoil deuteron does not get out of the target; here energy resolution alone distinguishes between the elastic and inelastic events. In the intermediate range (67°–106° c.m.) the proton is still identified by energy analysis but with its recoil deuteron in coincidence; the lower limit on the angle is determined by the necessity of the deuteron leaving the target with enough energy to be detected, the upper limit by constructional design difficulties in going to greater than 75° in the laboratory system (106° c.m.). In addition, energy of the deuteron was measured with the recoil proton in the range 80°–140° c.m.; the lower limit is again determined by the low energy of the deuteron, the upper limit by the low energy of the

[16] A. E. Taylor and E. Wood, Proc. Phys. Soc. (London) **A69**, 645 (1956); A. E. Taylor, E. Wood, and L. Bird, Nuclear Phys. **16**, 320 (1960).
[17] J. N. Palmieri, A. M. Cormack, N. F. Ramsey, and Richard Wilson, Ann. Phys. **5**, 299 (1958).
[18] C. Hwang, T. R. Ophel, E. Thorndike, and Richard Wilson, Phys. Rev. **119**, 352 (1960).
[19] E. Thorndike, J. Lefrançois, and Richard Wilson, Phys. Rev. **119**, 362 (1960).
[20] A. Kuckes and Richard Wilson, Phys. Rev. **121**, 1226 (1961).
[21] L. Wolfenstein, Ann. Rev. Nuclear Sci. **6**, 43 (1956).
[22] V. O. Nicolai, Rev. Sci. Instr. **24**, 618 (1955).

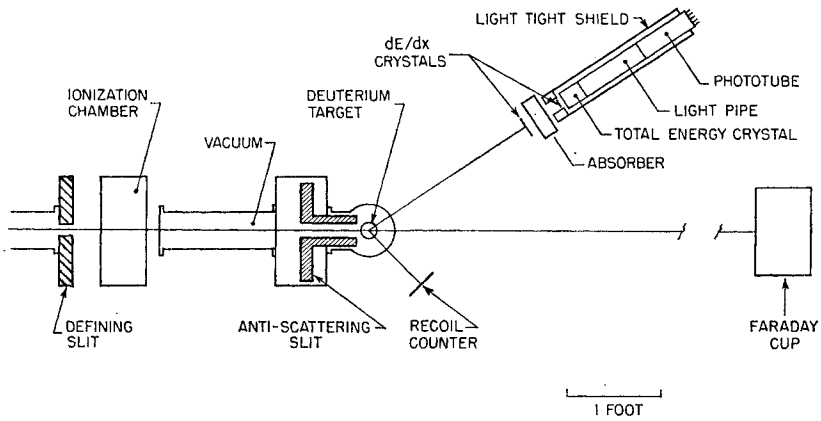

FIG. 2. Experimental arrangement.

proton. Finally at large angles (99°–170° c.m.) the deuteron energy alone was measured, relying on good energy resolution and a high rejection of protons to distinguish the elastic peak. This flexibility in detection makes it possible to cover the entire angular range, even to the extent of overlapping methods in some regions.

Some particles that are counted as elastic events from the deuterium target actually arise from other processes. One such background source results from scattering by target supports, slits, and air; its effect is found by emptying the target and counting the contribution to the elastic events. Corrections to the observed counts are necessary because the background particle has scattered with a higher energy and with a lower cross section than is the case when the target is full. After these slight adjustments the background is subtracted from the target-full events.

The background source caused by inelastic events is present only when there is a target and thus cannot be measured in the absence of the target; this negates the direct subtractive method that was possible above. This background is of particular concern when the protons are the particles of interest. The origin of one type of inelastic process is the "free *p-p* like" and "free *p-n* like" collisions in which the deuteron breaks up with the resulting collision partners exhibiting two-body nucleon-nucleon kinematics.[3] The unique angular and energy correlation of the analogous free case is disrupted in these quasi *p-p* and quasi *p-n* collisions by the internal momentum possessed by the struck particle in the deuteron at the time of impact. Experiments show that the inelastic and elastic processes here have cross sections of the same order of magnitude[23]; this, coupled with the fact that the inelastic particles are weakly correlated about angles different from the strong correlation of the elastic *p-d* events, again emphasizes that the use of a recoil counter in coincidence with a total energy detection system with good energy resolution will help greatly in the separation of elastic processes from this inelastic background. The incident proton may also cause an inelastic scattering in which the proton in the deuteron flips its spin to form a virtual deuteron with a "binding" energy of −70 kev. The proton being scattered in this fashion has been reduced in energy by 2.23 Mev in order to break up the real deuteron and by an additional 0.070 Mev to form the virtual deuteron; its energy is then 2.30 Mev below that of the elastically scattered proton. To experimentally separate the elastic and inelastic events a resolution of at least 2.30 Mev out of 146 Mev is needed. Even better resolution is necessary to distinguish a small inelastic scattering in the presence of a large elastic peak. The inability to achieve the necessary resolution to identify this effect is one of the uncertainties in the elastic results.

The main contribution to a background for the deuteron detection are the inelastic protons that may "break through" when the rejection of the discriminator apparatus is not adequate to prevent subsequent analysis of the detected proton. It is necessary then to design the equipment to have a high rejection ratio for protons to deuterons of the same energy when it is desirable to analyze the scattered deuteron. Since there are no inelastic deuterons possible this source of background may be discounted as a source of correction.

The result of these resolution requirement and flexibility of detection was a particle "telescope" of the form displayed in Fig. 2, together with the electronic circuits shown in the block diagram of Fig. 3. Whenever a particle loses a preselected amoung of energy in each of two "rate of energy loss" counters and then loses all of its remaining energy in the total-energy counter, pulses from these three events enter a fast coincidence circuit; the resulting triple coincidence assures the remaining electronic circuits that one particle of desired charge and mass is to be energy-analyzed. Also from the total-energy counter a fast pulse (30 nanoseconds) proportional in height to the particle's total energy passes through a cathode follower, down a delay line, and into a "gate and stretcher." Here the triple coincidence pulse (quadruple if we also require the defined particle's recoil partner in angular correlation) opens

[23] Arthur Kuckes, thesis, Harvard University, 1959 (unpublished).

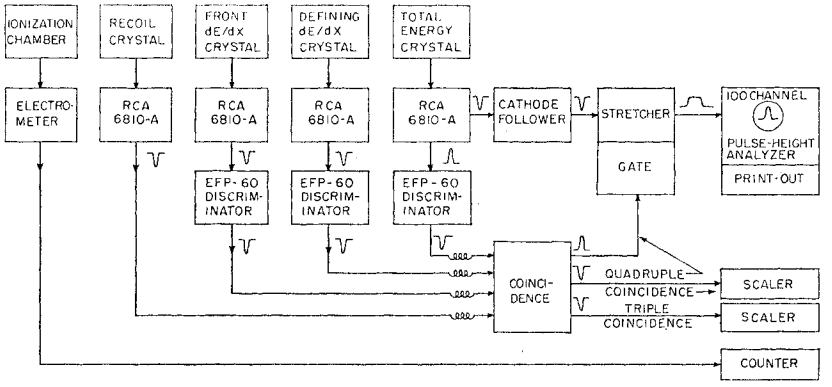

FIG. 3. Block diagram of electronic circuits.

the "gate" of 200-nanosecond duration which permits the fast pulse to enter the "stretcher," where it is stretched in time duration to 1.5 μsec but maintains its height. Finally, this lengthened pulse enters a 100-channel pulse-height analyzer where it is analyzed, displayed, and recorded in a channel corresponding to the initial scattered particle's energy.

The "rate of energy loss" counters give pulses whose height is proportional to the energy lost by the particle in passing through the scintillator. The discriminator units[24] reject all pulses below a predetermined height; the accepted pulses are uniformly shaped and continue to the coincidence circuit through appropriate delay lines.

The second rate of energy loss counter is also the "defining" counter, and its detection area of $\pi/4$ square inches together with the distance from the center of the target determines the solid angle of the experiment and the angular resolution. A deuteron loses 1.76 times as much energy as a proton of the same initial energy so distinction between the particles can be accomplished by discrimination between their pulse heights. For one discriminator the "feed through" ratio for protons to deuterons of the same energy is 3%. Requirement of two such identifications, reduces this ratio to 0.1%; in addition, these two counters reduce "accidental" rates and form a telescope to define the target region.

The total-energy scintillator is thick enough to stop the most energetic deuteron (130 Mev) but can only completely stop a 90-Mev proton. However, it is of large enough diameter to prevent most outscattering of both kinds of particles. To energy-analyze higher energy protons, it is necessary to slow them down to less than 90 Mev by placing CH_2 absorber between the front and defining crystals. A longer counter would have stopped the full-energy proton, but this larger volume becomes a better neutron detector; to reduce singles rates in the total-energy counter for better detection of deuterons, it is desirable to keep the volume small.

Good energy resolution in the telescope system is dependent upon the initial beam energy spread, the energy smear in the target, and the "inherent" resolution in the total-energy crystal and associated electronic circuits. The initial beam had a 3-Mev full energy width at half height at 148 Mev. This imposed an ultimate resolution of at least 2% on the apparatus. The energy smear in the target was negligible (less than $\frac{1}{2}$ Mev) for protons at small lab angles but for deuterons even at small laboratory angles the smear was 3 Mev. The final resolution was 3% for deuterons and 2.2% for protons in the scattered beam at small angles. The resolutions become worse at larger laboratory angles consistent with the increased energy smear in the target.

Beam Monitoring

Both the determination, the number of protons per integrated beam unit, and the monitoring of the beam were accomplished by the collection of the proton beam of a Faraday cup and electrometer.

An argon-filled ionization chamber placed in front of the target acted as an alternative monitor. The ionization chamber served as the primary monitor for angles less than ten degrees; the integrated ionization chamber current per integrated beam unit was found frequently in that case to provide an absolute calibration. The ionization chamber and the Faraday cup agreed to within $1\frac{1}{2}$%.

EXPERIMENTAL PROCEDURE

The 70% polarized proton beam of the Harvard cyclotron is obtained by internally scattering the regenerated beam from a 12-Mev thick carbon target. These polarized protons exit into an evacuated beam pipe at an approximate angle of 17° to the initial beam with 148-Mev energy, with 3-Mev full width at half-height energy spread, and with an intensity of 3×10^6 protons/sec.

To avoid introducing false asymmetries into the data of the polarization determination, the zero angle was carefully found by taking the beam profile and centering the defining crystal within this profile. The pivot of the radius arm about which the telescope

[24] J. J. Thresher, C. P. Van Zyl, R. G. P. Voss, and R. Wilson, Rev. Sci. Instr. **26**, 1186 (1955).

swung was positioned directly under the center of the target and the levelness of the scattering table adjusted so that there was no difference on either side of the zero beam line.

After the data was taken on one angle, the telescope was immediately swung to the same angle on the other side; the process was generally repeated once more. Also in covering an angular range the various angles were interleaved. Backgrounds were taken before and after filling the target for each angle in the experiment. These backgrounds were counted for only a fraction of the time of the target-full counting cycles; this fraction depended upon the importance of the background and varied in practice from $\frac{1}{8}$ to $\frac{1}{2}$.

EXPERIMENTAL AND ANALYTICAL CORRECTIONS

Dead Time

Counting losses occur when pulses appear within the time it takes an electronic circuit to perform an operation on one pulse and recover sufficiently well to perform the same function on another pulse; the effect of this "dead time" on the counting losses entered as a correction to the data. The time limit on analyzing ability meant that only one event per beam pulse (one event every 4 milliseconds) could be sorted according to its pulse height. The dead time correction to the data was applied at all angles to the background as well as to the target-full data; the largest correction (at 2.5°) was $12\pm1\%$. This correction was much smaller for all other angles and generally was less than 1%. Dead times in the discriminators and the coincidence circuit caused no trouble.

Calculated Nuclear Absorption Corrections

"Nuclear absorption" is a generic term that applies to any process which removes particles from the particular energy range of interest, the elastic peak for instance. Several ways of finding this attenuation are possible. The nuclear absorption can be calculated for protons and deuterons as a function of the amount of absorber from theoretical or measured cross sections. For protons it is possible to measure the attenuation directly in the proton beam. The attenuation for deuterons can be measured by a comparison of two separate measurements of the scattering cross section at a given angle; the number of elastic events in the energy-analyzed peak which undergoes strong nuclear absorption in the total-energy crystal, and the number of elastic events as determined by angular correlation in which there is almost no nuclear absorption.

Removal of an elastically scattered particle from its rightful place in the elastic peak may be caused by the particle not being detected at all because it has undergone a scattering while slowing down that resulted in a large deflection outside the detector's observation. An inelastic collision causes a reduction in energy so large that although the particle may still be detected it has fallen out of elastic recognition.

Single and plural Coulomb out-scattering losses are compensated almost entirely by the gain of particles from the in-scattering by the same processes. All particles that underwent inelastic scattering in the detection telescope were considered lost to the elastic peak. The proportion of elastic scattering by the absorber material that exceeded the geometrical confines of the detectors were also considered missing.

The method of calculation of this correction for proton detection is similar to that in reference 17. The corrections are greater than in that case, for we count as lost to the detector all particles that lose more than 4 Mev of their energy.

Unlike the case for the protons an absorber was not necessary to slow down the deuterons, and all nuclear absorption integrations were confined to the detectors. The calculations necessary for the deuterons were similar in form to those for protons; however, less well-known cross sections had to be used due to a lack of experimental information. The elastic scattering of the deuterons from hydrogen and carbon resulted in only small losses because the rate of energy loss of the deuteron was so high that such a scattered particle could not leave the thick total-energy crystal. Such scattering is concentrated in a small forward cone and the energy reduction is small. The deuteron-proton cross section has been reported for only one energy (190 Mev) and had the value of 53 mb/sr or 6% of the total cross section. Following Teem,[14] the cross section can be related to the more familiar total neutron-deuteron cross section at half the energy; $\sigma_{dp}(E)=0.75\sigma_{nd}(E/2)_{\text{total}}$. As in the case for the proton inelastic cross section from carbon, the deuteron-carbon inelastic cross section was assumed to be constant; and since the total-energy detector was in poor geometry just as it was for the reported cross-section measurement, the value of 0.667 barn could be used. The integrations were again performed numerically to account for changing cross sections with energy.

The results of these calculations for protons and deuterons for the incident energy and absorber combinations used experimental conditions are listed in Table II. Also in the same table are the experimentally measured corrections. Due to the lack of good cross-section measurements for the parameters of interest and due to simplifying assumptions made to facilitate calculations, the attenuations for deuterons may be in error by 10%; for protons by 3%.

Measured Nuclear Absorption Corrections

For protons it was possible to measure the nuclear absorption correction for almost all the scattered energies and absorber combinations used in the actual experiment. For the deuterons such a measurement was confined to one experimental situation.

TABLE II. Nuclear absorption correction factors.

ϕ Deut. lab angle	E_d Deut. energy Mev	Calc. deut. corr. factor	Meas. deut. corr.	Proton lab angle	E_p Proton energy Mev	CH_2 abs. gm/cm²	Calc. proton corr. factor	Meas. proton corr. factor
...	...	...	...	2.5	144	9.57	1.360	...
5	129.5	1.350		5.0	143	9.57	1.352	...
10	126.4	1.337		10.0	141	9.57	1.345	...
15	121.5	1.320		15.0	139	9.57	1.335	...
20	114.8	1.292		20.0	135	7.77	1.315	1.33±0.04
25	106.5	1.257		25.0	129	6.42	1.296	1.33±0.04
30	97.0	1.225		30.0	123	6.42	1.270	1.30±0.04
35	86.6	1.190		35.0	117	4.32	1.237	1.27±0.04
40	75.5	1.157	1.186±0.092	40.0	110	4.32	1.217	1.26±0.04
45	64.1	1.125		45.0	103	3.34	1.196	1.22±0.04
...	...	...	...	50.0	95	3.34	1.176	1.21±0.04
...	...	...	...	55.0	88	...	1.166	1.18±0.04
...	...	...	...	60.0	81	...	1.150	1.15±0.03
...	...	...	...	65.0	73	...	1.136	1.14±0.03
...	...	...	...	70.0	66	...	1.115	1.12±0.03
...	...	...	...	75.0	60	...	1.110	1.11±0.03
...	...	...	...	80.0	54	...	1.095	1.10±0.03

To measure the proton attenuation the telescope was placed in the direct beam and the same adjustment made as for the scattering experiment. A lead scatterer was placed over the pivot to scatter the beam so that the detection counters would be uniformly illuminated, and a CH_2 absorber was placed behind this scatterer to reduce the beam energy to that of the scattered particles of interest. Another large counter was placed before the front discriminator; these two acted as a monitor in double coincidence. As the beam energy was varied by changing the absorbers behind the radiator to simulate the scattered particles, the absorber between the front discriminator and the defining counter was varied with energy in the same manner as was done in the experiment. The number of triples and peak counts per monitor was noted for this latter absorber in and out. In this manner it was possible to separate the effects of the nuclear absorption in the absorber and in the total-energy counter: the former being the ratio of triples with the absorber out to that with it in. The total-energy counter and absorber effects combined was found by noting the ratio of the number of counts under the peak with the absorber in to the triples with the absorber out—all taken for the same number of monitor counts.

The ratio of the cross section measured by angular correlation to that measured by counts under the elastic peak in the total-energy crystal gave the attenuation of the deuterons at a particular angle and therefore particular energy incident on the total-energy counter. The angular correlation cross section is subject to small corrections for its nuclear absorption because only the discriminator counters are effective in absorbing the deuterons.

The experimental corrections for all proton energies and the single deuteron energy are given in Table II in the form of multiplicative corrections. The protons factors may be in error by 3% because of unknown low-energy contaminants in the beam and nonuniform illumination over the crystals. The lone deuteron measurement is probably in error as much as 8% due to the large uncertainty in subtracting by extrapolation of the neighboring inelastic particles. Comparison of both calculations and measurements of these attenuation factors with those of Teem and Palmieri whenever the same energy and absorber combinations were used show close agreement. Such a comparison was possible for six values for the protons and for all the deuterons below 95 Mev. Nuclear absorption corrections were made only to the cross section; the polarization was little affected by these processes. To correct for this effect, the experimental attenuation factors were used where possible for the proton cross section and the calculated ones for the deuteron cross section.

Beam Polarization Measurement

The desired polarization of the protons scattered from deuterons is related to the measured asymmetry and beam polarization by $P_{pd}=e_{pd}/P_B$. The separate calibration of the beam polarization by scattering from carbon at 15° gave a value of 70±3%. Then to find the polarization for a 100% incident beam it was necessary to divide the measured asymmetry by this 70%. It is to be noted that the correction to the 100% polarized incident beam is in error by 3%. This error was not included in the relative polarization error; it is necessary for an absolute determination of the polarization.

Scattering Angle and Azimuthal Corrections

The finite size of the defining counter necessitates slight correction of the small angle measurements. Because the cross section at small angles varies very rapidly, close to θ^{-4}, the portion of the detector closest to the beam counts more particles than its far side.

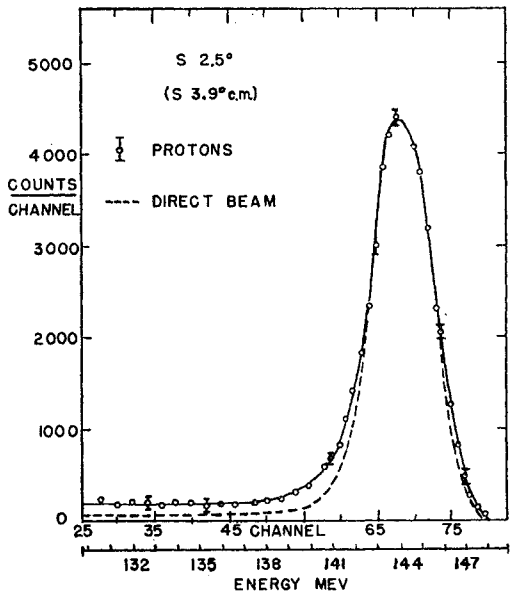

FIG. 4. Pulse-height distribution of protons at $2\frac{1}{2}°$ lab (3.9° c.m.).

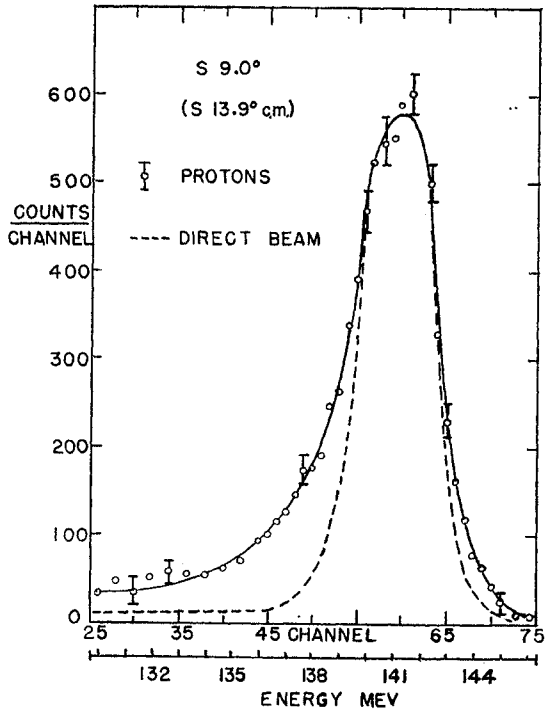

FIG. 5. Pulse-height distribution of protons at 9° lab (13.9° c.m.).

Thus the effective scattering angle is smaller than the nominal angle measured by displacements on the sine bar. On the other hand, because the beam also possesses a vertical dimension, some particles are further away from the nominal center and this tends to make the effective angle larger. The correction was important for 2.5° and 3° lab angles and changed them to 2.46° and 2.98°, respectively.

A correction to the polarization is necessary because the counter detects scattering which is out of the plane normal to the direction of polarization. This correction was 0.7% at 2.46°, becomes smaller at larger angles, and was neglected in all regions.

All corrections are subject to errors either in the method used, assumptions made in the calculations, or in the data used to attain the final numerical results. In all cases, the corrections were made to the data and the errors acknowledged by including them in the total errors of the experiment.

Data Reduction

Corrections to the data have been made for the dead time of the pulse-height analyzer, the scattering when the target was empty, and the inelastic scattering from the deuteron. The target-empty background was only appreciable from $2\frac{1}{2}°$ to 10° lab. A correction was made to the target empty data for energy loss in the deuterium and the counts subtracted channel by channel.

The background of protons scattering inelastically from the proton leaving the deuteron in the 2–3 Mev virtual state are important at small angles. The resolution of 3 Mev full width at half maximum was inadequate to separate these completely as shown in Figs. 4 and 5. The dashed curve shows the spectrum of protons taken in the direct beam with the peak position and intensity normalized. A group of inelastically scattered protons is easily seen to distort the peak. At $2\frac{1}{2}°$ lab the distortion is small, because the elastic Coulomb scattering is large, and the inelastic scattering negligible. The number of elastically scattered protons have been estimated by taking only the counts on the high-energy side of the peak and doubling them. This procedure reduces the effect of the inelastically scattered protons to less than 5% at all angles. At these angles, the total counts integrated over the elastic and inelastic scattering up to 5-Mev energy loss, are also presented. A study[25] in progress with a magnetic spectrometer of 1% resolution separates the elastic and inelastic data.

Incorrect accounting for the inelastically scattered protons can cause a systematic error both in the cross section and polarization.

At larger angles, 25° lab (Fig. 6) the target empty background is small, but the inelastic background becomes so large that the elastic scattering peak need not be symmetrical. The excitation of the 2.3-Mev state, being magnetic dipole, may be assumed small. The dotted lines in Fig. 6 show two extreme ways of accounting for the inelastic events. The systematic error in subtracting the inelastic contribution was obtained from these two extremes. At 50° lab (Fig. 7) the situation is even worse. The c.m. cross section there becomes 0.60 ± 0.10 mb/sr and the polarization

[25] D. Stairs (private communication).

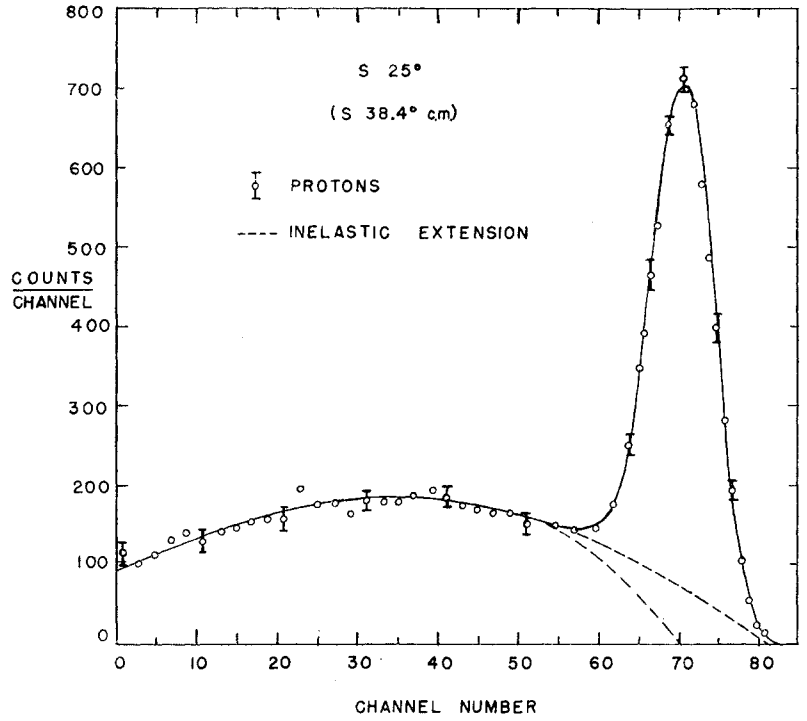

FIG. 6. Pulse-height distribution of protons at 25° lab (38.4° c.m.).

-0.24 ± 0.06. However it is now possible to count deuterons in recoil and thus completely specify the kinematics. The background vanishes, except for a small tail due to nuclear absorption in the counter, and the errors reduce; using this method the cross section becomes 0.58 ± 0.05 mb/sr and the polarization -0.30 ± 0.05.

Figures 8 and 9 exhibit data taken at 40° lab by three different methods: the deuterons energy analyzed with no recoil required, the deuterons energy analyzed with the recoil proton required, and the deuteron identified in the telescope with the proton recoil counter swept through several angles to provide an angular correlation measurement. The background is inelastically scattered protons feeding through the electronic circuits.

Figure 10 exhibits the data of energy-analyzed deuterons taken on the right-hand side of the beam at 10° lab. The solid line represents an estimate of the

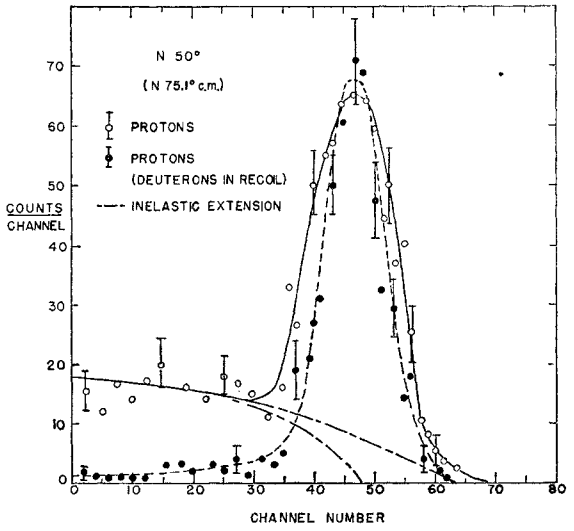

FIG. 7. Pulse-height distribution of protons at 50° lab (75.1° c.m.).

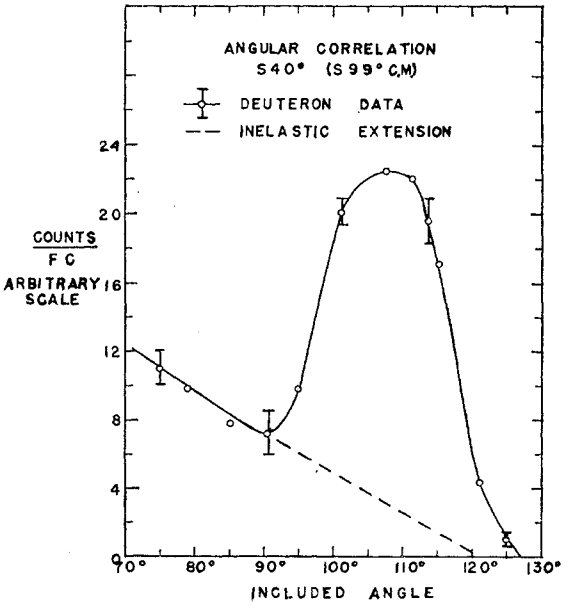

FIG. 8. Angular correlation of coincidences at 40° lab (99° c.m.).

best fit through the raw experimental data. The elastic peak is here distinctly separate from the quasi-elastic background. An estimated correction for the proton feed through is very small (0.5%). The elastic peak was symmetric and exhibited no influence from the presence of inelastic particles. The backgrounds for the target empty also were very small and did not warrant the channel by channel subtraction necessary in the case of small-angle proton analysis.

TABLE III. Elastic p-d scattering results.[a]

Center-of-mass angle (deg)	Lab angle (deg)	Det. method	Center-of-mass cross section $(d\sigma/d\omega)$ (mb/sr)	Polarization P	θ_{res} c.m.
3.9	2.5	p	114.60±10.49	0.083±0.058	±1.0
4.7	3.0	p	42.64±3.86	0.207±0.039	±1.0
6.3	4.0	p	17.95±1.63	0.287±0.027	±1.0
7.7	5.0	p	14.24±1.29	0.252±0.026	±1.0
9.3	6.0	p	17.87±1.62	0.290±0.026	±1.0
10.9	7.0	p	18.36±1.66	0.309±0.026	±1.0
12.4	8.0	p	16.06±1.45	0.332±0.026	±1.0
13.9	9.0	p	16.64±1.51	0.369±0.026	±1.0
15.5	10.0	p	16.46±1.49	0.406±0.026	±1.0
19.3	12.5	p	11.93±1.67	0.428±0.063	±2.2
23.1	15.0	p	10.45±1.62	0.550±0.057	±2.2
30.8	20	p	5.40±0.46	0.681±0.034	±2.2
38.4	25	p	3.64±0.36	0.676±0.031	±2.2
45.8	30	p	2.36±0.23	0.512±0.030	±2.2
53.2	35	p	1.70±0.17	0.278±0.036	±2.3
60.4	40	p	1.14±0.12	0.075±0.046	±2.4
67.5	45	p	0.906±0.119	−0.179±0.053	±2.4
75.1	50	p	0.602±0.102	−0.236±0.060	±2.6
75.1	50	p, d	0.584±0.047	−0.299±0.047	±2.6
81.3	55	p, d	0.492±0.049	−0.416±0.050	±2.7
87.6	60	p, d	0.390±0.039	−0.429±0.049	±2.8
93.9	65	p, d	0.335±0.034	−0.497±0.047	±2.9
105.7	75	p, d	0.263±0.042	−0.623±0.056	±3.0
99	40	d, p	0.263±0.026	−0.639±0.061	±3.2
99	40	d	0.274±0.054	−0.739±0.082	±3.2
109	35	d	0.245±0.040	−0.592±0.098	±3.1
120	30	d	0.235±0.034	−0.488±0.105	±3.0
130	25	d	0.247±0.030	−0.044±0.067	±3.0
140	20	d	0.280±0.031	0.116±0.042	±2.9
150	15	d	0.326±0.033	0.178±0.051	±2.8
155	12.5	d	0.406±0.050	0.235±0.058	±2.8
160	10	d	0.477±0.038	0.173±0.047	±2.8
165	7.5	d	0.582±0.068	0.090±0.056	±2.8
170	5.0	d	0.795±0.097	0.112±0.056	±2.8

[a] "Det. method" is the detection method used: p is the proton energy analyzed, d is the deuteron energy analyzed, p, d is the proton energy analyzed with deuteron in recoil, and d, p is the deuteron energy analyzed with proton in recoil. θ_{res} is the angular resolution expressed in the center-of-mass system.

Errors

Most of the errors and the method of accounting for them have already been mentioned in a number of scattered places. For the sake of completeness they are collected here: the statistical fluctuation in the number of counts in the peak, the statistical fluctuation in the number of counts in the target-empty background subtractions, the statistical fluctuation in the number of counts in the inelastic subtraction; the uncertainty in inelastic subtraction; the error in finding the number of target atoms, the beam intensity, and the solid-angle

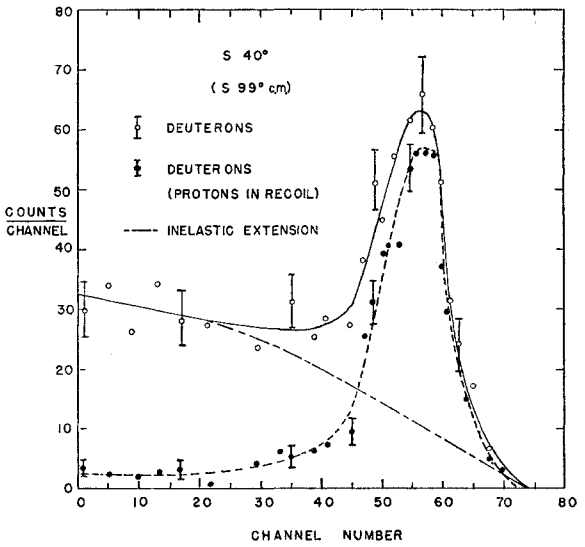

FIG. 9. Pulse-height distribution of deuterons at 40° lab (99° c.m.).

errors in the correction factors for dead time, multiple scattering, background cross section, and energy shift, nuclear absorption—all these have been given in some detail previously. What remains for further investigation are the errors introduced by pivot misalignment, uncertainty in zero-angle determination, and uncertainty in the scattering angle.

Alignment errors have a total effect of introducing a false polarization of ±0.05 at the 2.5° angle. At all

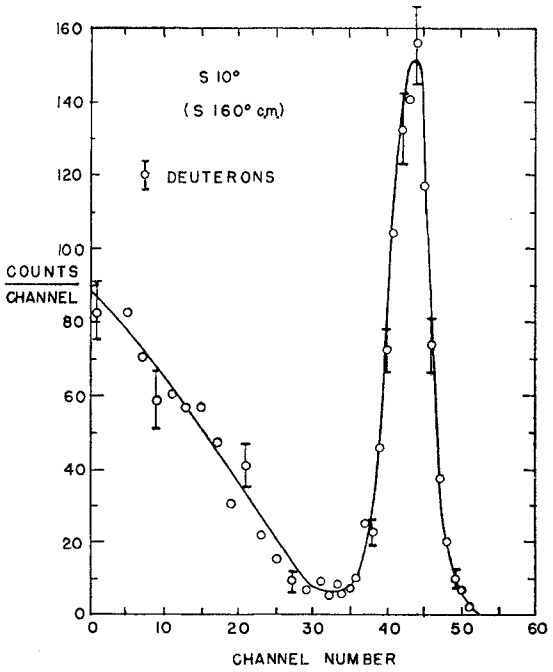

FIG. 10. Pulse-height distribution of deuterons at 10° lab (160° c.m.), showing inelastic proton feed through.

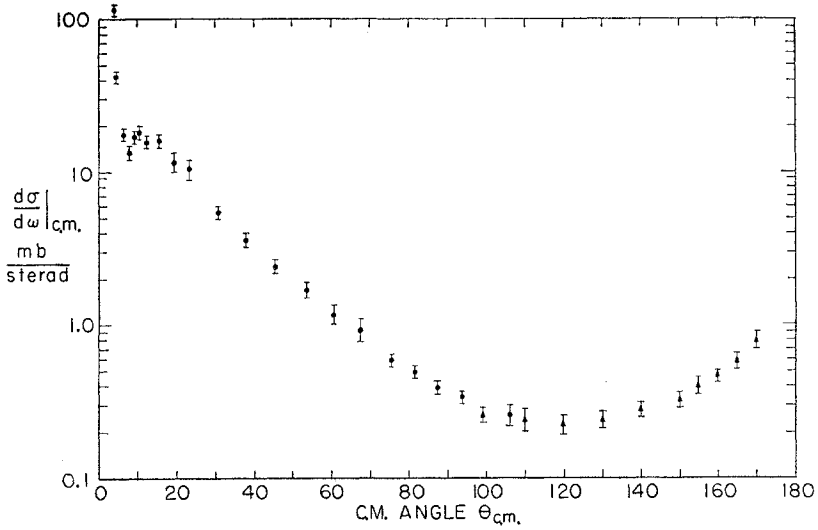

FIG. 11. Cross section for p-d elastic scattering at 146 Mev.

other angles, the effect is much smaller, dropping to a typical value ± 0.008 at 15°.

False polarizations from azimuthal deviations can arise from the uncertainty in positioning the center of the defining crystal at the height of the scattering plane or from variations in the height of the scattering table. The combined uncertainty from these two effects was less than $\frac{1}{8}$ in. which could lead to a false polarization of 0.007 at 2.5° where such an effect would be most pronounced.

The experimental polarization and cross sections are given in Table III. It must be emphasized that the errors are largely systematic (mainly arising from the uncertainty in the inelastic subtraction), and that while the values given for the errors in Table III represent the estimated limits, the "correct" values for the polarization and cross section may lie close to either limit; therefore, although the curves of Figs. 11 and 12 retain their shapes, they may be displaced slightly upward or downward to either extreme of the indicated errors as far as this experiment can determine.

The large errors arising from the uncertainty in the inelastic subtraction are caused mainly by poor resolution; this may be solved by reducing the initial beam energy spread, the target thickness, and the inherent resolution of the detection system. The errors in the nuclear absorption correction are best eliminated by eliminating the necessity for making a nuclear absorp-

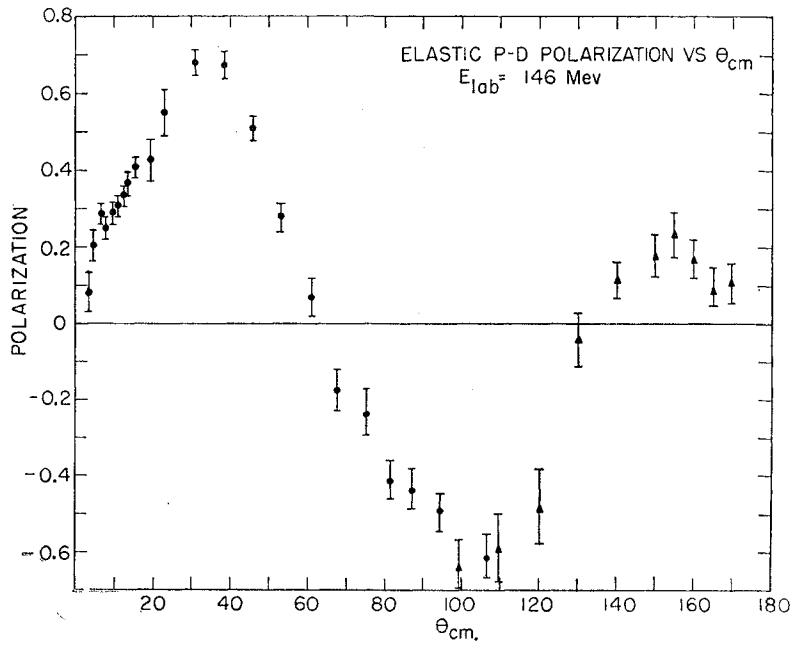

FIG. 12. Polarization or asymmetry in p-d elastic scattering at 146 Mev.

tion correction at all. This too involves a change in the detection system because the correction was a result of using the total energy detection method. After a beam of high intensity and small energy spread has been obtained, and a smaller target designed, then the detection apparatus would have to be a magnetic spectrometer in order to maintain good resolution. The limit of the resolution using this method is determined by the regulation of the current supply to the magnet and the angular acceptance of the defining counter, of the order of 1% with ease. The limit to the resolution for detection by total energy analysis with plastic scintillators has been shown to be about 2%.

The final data for cross section and polarization are presented in Table III and Figs. 11 and 12.

Discussion

One may compare our cross section with those taken at other energies (see Fig. 13). All data are characterized by a forward maximum, a minimum near 130°, and a backward maximum in the pickup region. There is a basic disagreement between the cross section determined here and the one by Cassels *et al.*[7] at a similar energy. Cassels' cross section is higher than that measured here, and the shape is slightly different. No systematic checks were described by Cassels to test their statement that the inelastic contribution was small. Cassels' data were normalized to his p-p data. These p-p data were later found to be 25% too large. The combinations of these two effects may put Cassels' absolute p-d cross section 50% too high. Any reasonable plot of experimental cross section versus energy for a given angle also shows Cassels' data to be far out of line with the other energies. No comparison for energy variation of polarization is possible due to the lack of other polarization experiments. The data of reference 10 appeared only while the paper was in proof.

Several theoretical papers have been circulated[1] whose object is to combine the two-nucleon interactions in such a way as to predict the polarization and cross section for the deuteron. These theories are very similar in their assumptions, and their predictions are fairly close to one another; here the methods and predictions of Kerman, McManus, and Thaler (KMT)[1] are adopted because of their completeness. They represent a refinement of the calculations in reference 6.

The impulse approximation is made; the effects arising from multiple scattering, the effects of pickup (or exchange) scattering have been neglected; although the D-state contribution to the deuteron wave function is considered in a calculation of the form factor, it is usually neglected as far as its contribution to the scattering amplitudes is concerned.

The momentum transferred to the scattering particle by the incident particle is assumed to be the same as that transferred to the nucleus as a whole. The relation for the final momentum of the scattered particle k_f^2 as

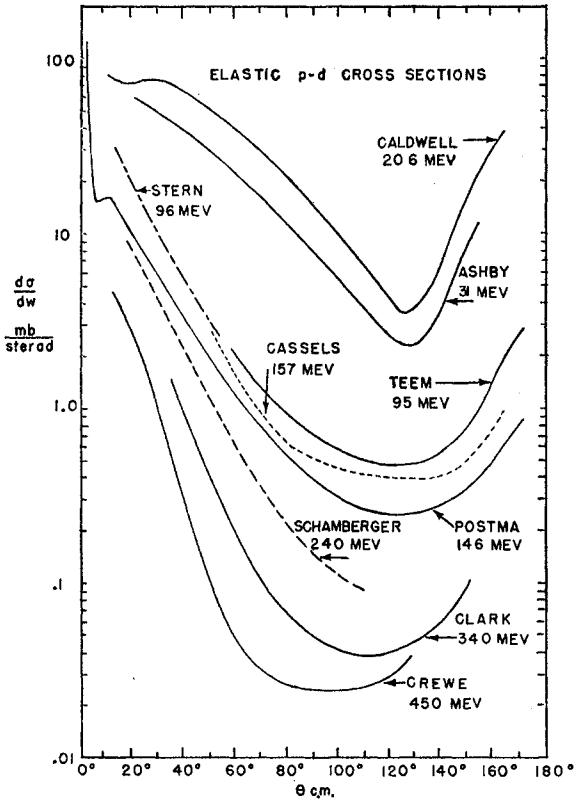

FIG. 13. Cross section for p-d elastic scattering at various energies.

a function of q^2 (the momentum transfer) and k_0^2 (the initial momentum) is a different functional relation in the two cases of nucleon-nucleon scattering and nucleon-nucleus scattering. In relating the quantities of interest for the nuclear scattering case to the nucleon-nucleon scattering amplitudes this different functional dependence is ignored, although the actual complex-nucleus scattering takes place "off the two-body energy shell." This assumption also neglects the momentum of the struck particle at the instant of impact. The assumption of neglecting off-the-energy-shell scattering is valid in the small-angle region.

These assumptions limit the theory to the small-angle region to predict the cross section and polarization with any accuracy. This small-angle region for the deuteron is less than 80° c.m.

The theory of KMT relates the nucleon-nucleus scattering matrix $\bar{M}(q)$ to the nucleon-nucleon scattering matrix $M(q)$ by averaging $M(q)$ over the target nucleons' spin and isotopic spin. $M(q)$ as a function of momentum transfer is written

$$M(q)=A(q)+B(q)(\boldsymbol{\sigma}_1\cdot\hat{n})(\boldsymbol{\sigma}_2\cdot\hat{n})+C(q)(\boldsymbol{\sigma}_1\cdot\hat{n}+\boldsymbol{\sigma}_2\cdot\hat{n}) +E(q)(\boldsymbol{\sigma}_1\cdot\hat{q})(\boldsymbol{\sigma}_2\cdot\hat{q})+F(q)(\boldsymbol{\sigma}_1\cdot\hat{p})(\boldsymbol{\sigma}_2\cdot\hat{p}), \quad (2)$$

where 1 is the incident nucleon, 2 is the scattering nucleon, and the unit vectors $\hat{n}$, $\hat{q}$, $\hat{p}$ are related to the

incident momentum $\mathbf{k}_0$ and final momentum $\mathbf{k}_f$ of the scattered nucleon by

$$\hat{n}=\frac{\mathbf{k}_0 x \mathbf{k}_f}{|\mathbf{k}_0 x \mathbf{k}_f|}, \quad \hat{q}=\frac{\mathbf{k}_f-\mathbf{k}_0}{|\mathbf{k}_f-\mathbf{k}_0|}, \quad \hat{p}=\frac{\mathbf{k}_f+\mathbf{k}_0}{|\mathbf{k}_f+\mathbf{k}_0|}; \quad (3)$$

$\hat{n}$ is a unit vector normal to the scattering plane, $\hat{q}$ is the momentum transfer unit vector, and with $\hat{p}$ they form a right-handed coordinate system for on-the-energy shell scattering.

The isotopic spin dependence is implicit in the scattering amplitudes A, B, C, etc. through the relation

$$A=\tfrac{1}{4}(3A_1+A_0)+\tfrac{1}{4}(A_1-A_0)\mathbf{T}_1\cdot\mathbf{T}_2, \quad (4)$$

where the subscripts 1 and 0 refer to the triplet and singlet isotopic spin states of T. The proton-proton scattering coefficient is A_1, and the neutron-proton scattering coefficient is $\frac{1}{2}(A_1+A_0)$.

The spin and isotopic spin average over the target nucleons gives the scattering matrix $\bar{M}(q)$; the scattering amplitude g_B in the Born approximation and the polarization P can be expressed in terms of this average through the relations

$$g_B(q)=\frac{2N}{N+1}N\bar{M}(q)F(q); \quad \frac{d\sigma}{d\omega}(q)=g_B{}^2, \quad (5)$$

$$P(q)=\frac{\mathrm{Tr}[\bar{M}(q)(\boldsymbol{\sigma}\cdot\hat{n})\bar{M}^\dagger(q)]}{\mathrm{Tr}[\bar{M}(q)\bar{M}^\dagger(q)]}, \quad (6)$$

where g_B and $d\sigma/d\omega$ are in the center-of-mass system of the nucleus, N is the number of nucleons in the target nucleus, and $F(q)$ is the nuclear form factor (the Fourier transform of the nucleon density in the ground state of the nucleus) which can be measured by electron scattering experiments. When this experimental measurement is used, the form factor for the proton must be subtracted out because the theoretical form factor assumes that the protons are point charges.

These quantities may be evaluated explicitly for the elastic scattering from the deuteron. The ground state is assumed to be entirely S-state with isotopic spin 0, spin 1, and total nuclear spin of 1. The result is

$$\frac{d\sigma}{d\omega}(q)=g_B{}^2=\left(\frac{2N^2}{N+1}\right)^2[A^2+C^2+\tfrac{2}{3}(B^2+C^2+E^2+F^2)F(q)^2], \quad (7)$$

$$P(q)=\frac{2\,\mathrm{Re}(A^*C+\frac{2}{3}B^*C)}{A^2+C^2+\frac{2}{3}(B^2+C^2+E^2+F^2)}, \quad (8)$$

where the average over isotopic spin has simplified A, B, C, etc., to the form $A(q)=\frac{1}{4}[3A_1(q)+A_0(q)]$, etc.

KMT supplied along with this theory the values of $A_1(q)$, $A_0(q)$, etc., for the energies of 90, 156, and 310 Mev. These values are related to the scattering amplitudes M_{ij} referring to the scattering of a nucleon-nucleon system from triplet spin component j to i and to the singlet scattering amplitude M_{22}; these in turn are related to the phase-shift solutions. The set of scattering amplitude coefficients $A_1(q)$, $A_0(q)$, etc., supplied by KMT was calculated from the phase shifts of Gammel-Thaler potential.

The values for the cross section and the polarization were calculated directly from these scattering amplitude coefficients using relations 7 and 8. But because the scattering amplitude coefficients did not include Coulomb effects, the values obtained were predictions for neutron-deuteron scattering. The form factor used in the calculation was taken from the experimental data of Stanford with the proton form factor unfolded.

To include Coulomb effects for proton-deuteron scattering, we follow a procedure and analysis of Bethe.[26] The scattering amplitudes for nuclear scattering of the proton magnetic moment in the Coulomb field may be added algebraically in the laboratory system.

In the Born approximation, the nuclear scattering amplitude in the lab system is

$$g_{\mathrm{BNL}}=2N\bar{M}(q)F(q). \quad (9)$$

In the Born approximation the Coulomb scattering amplitude in the lab system has the same form factor as the nuclear scattering and is

$$g_{\mathrm{BCL}}=2\frac{me^2}{\hbar^2q^2}e^{2i(\eta_c-\eta_p)}F(q). \quad (10)$$

The result for the Born approximation for the magnetic moment scattering amplitude in the lab system is

$$g_{\mathrm{BML}}=k\left(\frac{E_L-\mathrm{mc}^2}{mc^2}\right)(\mu-\tfrac{1}{2})\frac{q}{k_L}\frac{2e^2m}{\hbar^2q^2}e^{2i(\eta_c-\eta_p)}F(q), \quad (11)$$

where rest energy, is the charge of the incident proton, E_L and k_L are the total energy and momentum of the incident proton in the lab system, μ is the magnetic moment of the proton, $\eta_c-\eta_p$ is the difference in phase shifts applied to Coulomb and nuclear scattering, and the remaining symbols have retained their previous definitions.

If we assume that Coulomb and magnetic scattering are the same from a spin 1 as from a spin 0 nucleus, then the only scattering amplitudes influenced by their inclusion will be the A and C amplitudes. The average over the scattering amplitudes for a spin 0 nucleus gives

$$\bar{M}(q)=A+C\boldsymbol{\sigma}\cdot\hat{n}, \quad (12)$$

for the nuclear scattering amplitude in the Born approximation in the lab system

$$g_{\mathrm{BNL}}=2N[A+C(\boldsymbol{\sigma}\cdot\hat{n})]F(q); \quad (13)$$

and adding in the lab system the effects from (9) and

[26] H. Bethe, Ann. Phys. **3**, 190 (1958).

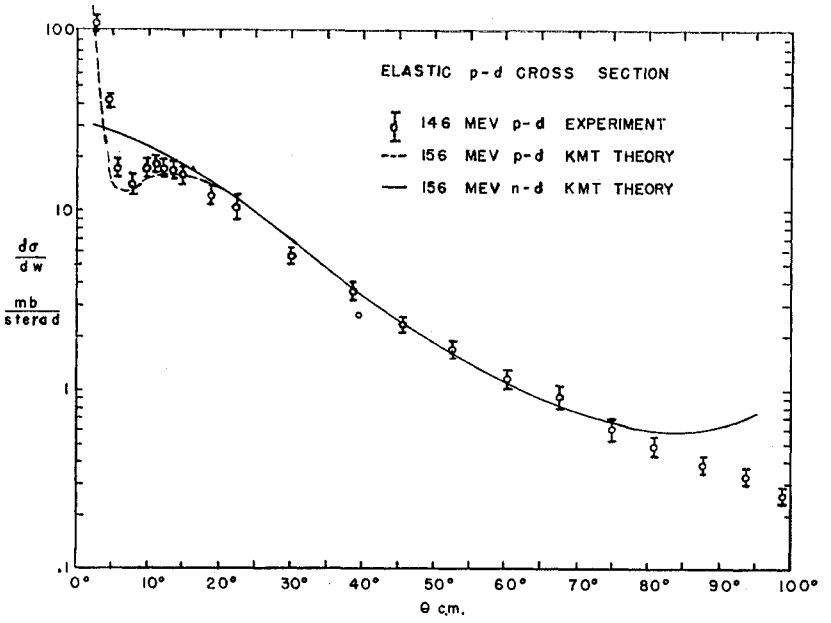

FIG. 14. Impulse approximation calculations for p-d and n-d elastic scattering cross section compared with experiment.

(10) gives

$$g_{\text{B total L}}=g_{\text{BNL}}+g_{\text{BCL}}+g_{\text{BML}}$$
$$=2N[A'+C'(\sigma\cdot\hat{n})]F(q). \qquad (14)$$

The newly defined scattering amplitudes A' and C' include the A and C of nuclear scattering and the effects of the Coulomb and magnetic moment scattering. The A' and C' were calculated and used together with the B, E, and F in 7 and 8 to calculate the cross section and polarization for proton-deuteron scattering.

The results from the calculation for p-d scattering were again in the momentum exchange representation which was changed to the lab or center-of-mass angle representation. Figure 14 shows the results of these calculations for the p-d and n-d differential cross section in the center-of-mass system together with the experimental points for the 146-Mev p-d scattering. The comparison between p-d theory and experiment is quite good in the range below 75° c.m., with the theory being at worst 10% different from the experiment. The theory rapidly departs from agreement for angles larger than 75°; this is probably a consequence of the assumptions pointed out earlier in this section breaking down. The calculations seem to differ from those of Fig. 3 reference 1. The reason for the difference is not clear.

Figure 15 shows the results of the calculations for the p-d and n-d polarization for the center-of-mass angles together with the p-d polarization found in this

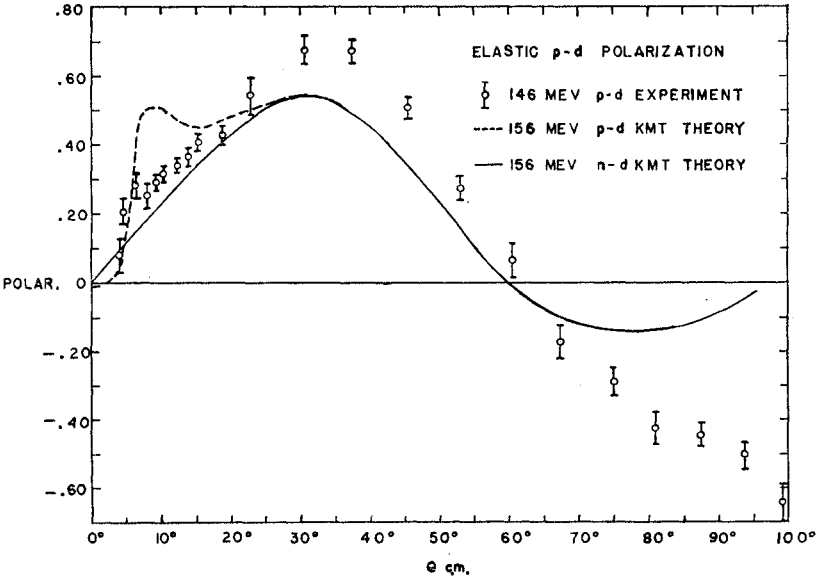

FIG. 15. Impulse approximation calculation for p-d and n-d elastic scattering polarization compared with experiment.

experiment. The comparison between theory and experiment here is good, but not as close as was the agreement for the cross sections. There is the expected deviation for angles larger than 75° because of the assumptions of the theory probably breaking down. However, in the Coulomb interference region there is a disagreement between theory and experiment. This is to be contrasted to the good fit obtained for cross sections. The reason for the disagreement in the polarization is not understood. There are also disagreements between experimental and theoretical polarizations at larger angles. The theory there predicts a polarization which is too small. The Gammel-Thaler potential gives too small a magnitude and a shift to the left in angle for its prediction to the experimental polarization for p-n at 146 Mev. Since the p-n polarization exhibits this effect, we may expect the same result to be maintained when the p-n scattering amplitudes are combined with the p-p to form a deuteron. This is a fault in the potential. The KMT theoretical prediction for p-α polarization at 146 Mev also displays a similar large angle disagreement[27]; however, in that case it is felt that the disagreement is a consequence of neglecting multiple scattering in the KMT theory. For the deuteron it is probably a combination of the failure of Gammel-Thaler potential to predict the p-n data closely and not including multiple scattering effects in the KMT theory.

The agreement between the KMT theory and experiment is generally quite good in the region where the assumptions are valid. It has similarly displayed success in predicting cross sections and polarizations in the elastic scattering from[27] He^4 and[28] C^{12} and for the inelastic scattering from the low levels of several other elements.

Pickup Scattering

Pickup takes place when an incident proton "picks up" a bound neutron to form a deuteron. The theory of this has been developed in impulse approximation by Chew and Goldberger.[2] Initial and final state interactions have been considered by Greider.[29] The Born approximation cross section depends on two factors; the probability that a neutron has a momentum k_n inside the nucleus and the probability that the neutron will interact with the incident proton to form a deuteron. If the momentum distribution of the neutron $\phi(k_n)^2$ is an unknown parameter, the experiment can in principle determine it. Qualitatively we see at once that small neutron momenta are more probable than large, and this will give a large forward peak of deuterons, or a peak in the p-d cross section near 180°. For the deuteron, the impulse approximation is more likely to be valid than for carbon nuclei where the theory has also been applied. However, the cross section of Eq. (7) is not zero in the pickup region; there will therefore be interference between the direct and pickup scattering. This has been discussed earlier by Teem.[14]

We first note the small positive asymmetry in the p-d elastic scattering from 140°–170° c.m. This corresponds to a negative asymmetry of the pickup deuteron from 5°–15° lab. In a study of pickup deuterons from carbon, $C^{12}(p,d)C^{11}$, Cooper[30] found no asymmetry of the deuterons at these angles, and a large positive asymmetry at larger angles. This was qualitatively explained by Greider in terms of the interaction of the incoming proton with the carbon nucleus; the Born approximation theory predicts no polarization, because a neutron is equally likely to have either sign of momentum.

We therefore tentatively attribute this asymmetry to interference between the direct and the pickup scattering. We must now consider the sign of this interference. The polarization changes sign very rapidly from 120° to 150° c.m. It is in this region also that the pickup process becomes dominant. We therefore attribute the change of sign of polarization to a destructive interference. If we examine the predictions of KMT (their Tables III and XIII) we see that the direct scattering could not by itself account for this change of sign.

Of course the destructive interference may not be complete. Equation (7) shows that the direct scattering amplitude has the five complex terms; interference is expected only with the first term A and the Born approximation suggests only with $\mathrm{Re}A$.

We have analyzed the data in two ways. Firstly, we assume that the direct cross section is negligible and therefore there is no interference. The p-d cross section then becomes

$$\frac{d\sigma}{d\omega}=\frac{16\pi^2}{3}\frac{(\beta^2-\alpha^2)}{(\alpha^2+k^2)^2(\beta^2+k^2)^4}, \tag{15}$$

or by substitution

$$\frac{d\sigma}{d\omega}=\frac{970}{1+0.1E_0(1+8\sin^2\phi)^2}\frac{26}{27+0.1E_0(1+8\sin^2\phi)}, \tag{16}$$

where E_0 is the incident proton energy in the lab system ϕ is the laboratory angle of the pickup deuteron. We have taken a Hulthén approximation to the deuteron wave function,

$$\psi(r)=\frac{0.191}{r}(e^{-0.232r}-e^{-1.202r}). \tag{17}$$

[27] A. M. Cormack, J. N. Palmieri, N. F. Ramsey, and Richard Wilson, Phys. Rev. 115, 599 (1959).
[28] E.g., P. Hillman, A. Johansson, and G. Tibell, Nuclear Phys. 4, 648 (1957). Also see reference 1.
[29] K. Greider, Phys. Rev. 114, 786 (1959), and University of California Radiation Laboratory Report UCRL-8357 (unpublished).
[30] P. F. Cooper, Jr., and Richard Wilson, Nuclear Phys. 15, 373 (1959).

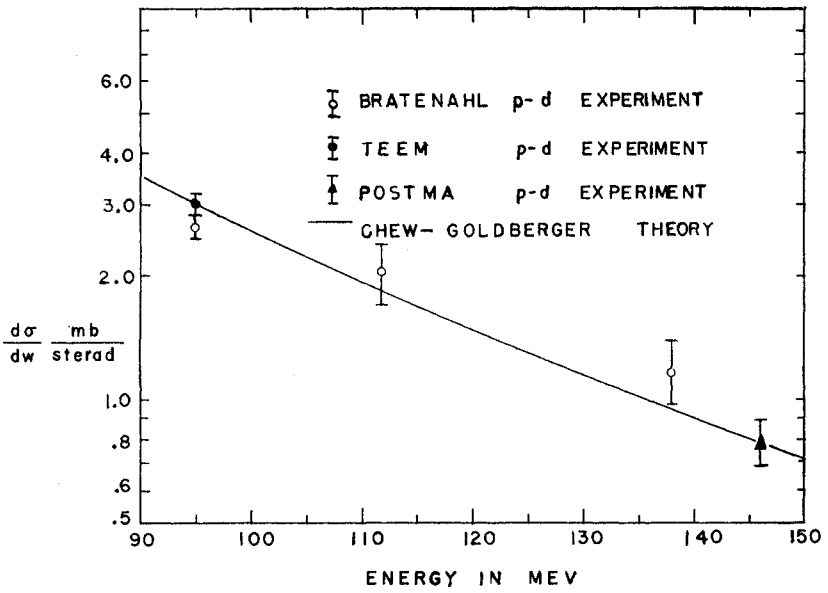

FIG. 16. p-d elastic scattering cross section in the pickup region (170° c.m.) as a function of energy compared with the simple Chew-Goldberger theory.

where r is in units of fermi$=10^{-13}$ cm. This fits the usual deuteron parameters—the binding energy and the effective range.

We do not obtain exact agreement with this cross section. We might expect neglected effects to be a multiplication factor in the cross section.

The theoretical results were therefore normalized to the experimental point of Teem[14] at 170° c.m. and 95 Mev with a multiplicative factor of 1.50. A part of this factor may also be due to the destructive interference between the direct and the pickup scattering. Figure 16 shows the experimental cross section of this experiment and that of Bratenahl[13] at the same angle. The agreement is good, showing that the energy dependence, and therefore dependence on neutron momentum k, of Eq. (15) is good. Figure 17 shows the calculated cross sections as a function of $\theta_{\text{c.m.}}$ for both 95 Mev and 146 Mev. The deviation at small θ may be due either to interference with direct scattering, to an inadequate deuteron wave function giving an incorrect neutron momentum distribution at high momenta, or to final-state interactions.

In order to gain some idea of the second of these, we have calculated the cross section with assumptions of complete destructive and complete constructive interference. The calculation follows that of Teem[14] though the notation differs.

The complete scattering cross section is written

$$\frac{d\sigma}{d\omega}(\theta)=F(\theta)\{A(\theta)+X\pm Y(\alpha^2+k^2)[\phi(k)]^2\}^2, \quad (18)$$

where the first term is from the KMT theory [our Eq. (7)] and is here assumed to be completely real and spin independent. The term X is a small constant term to take account of multiple scattering and exclusion principle effects. The third term is the Born approximation pickup term of Eq. (15) with an adjustable constant Y, the deuteron wave function in momentum space $\phi(k)$, and a sign to indicate complete constructive or destructive interference.

The first term, is smallest in the pickup region. At small θ it dominates and gives a cross section F^2A^2 which is a gross simplification of Eq. (7). A value can thus be assigned. Chew[14] estimated that the term $X^2=0.06$ mb/sr about 6% of the cross section at 180°. From this we may calculate $\phi(k)$ according to constructive or destructive interference. Figure 18 shows the result of such a calculation. The solid curves were obtained by Teem

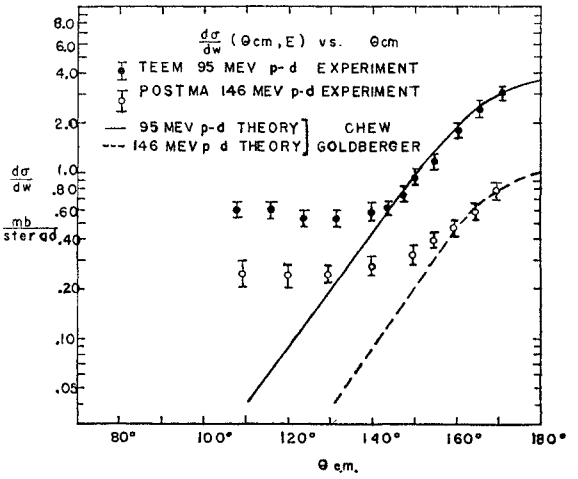

FIG. 17. Cross section in the pickup region as a function of angle compared with the simple Chew-Goldberger theory.

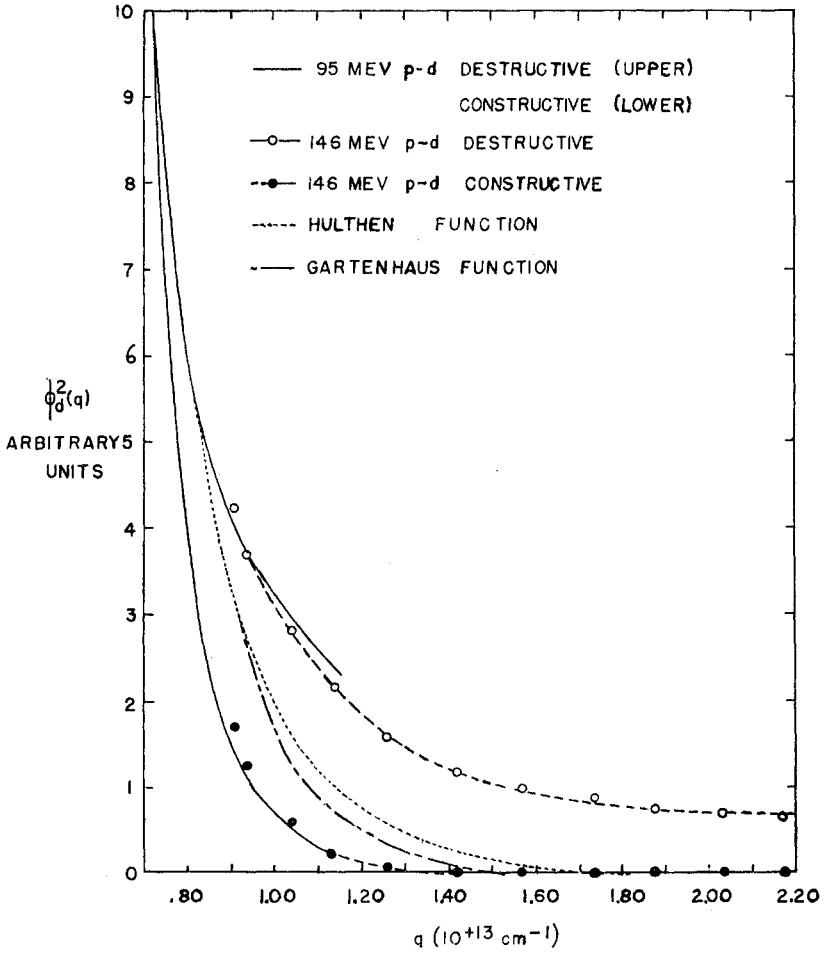

FIG. 18. The square of the deuteron wave function in momentum space ϕ_d^2 deduced from 95-Mev and 146-Mev deuteron pickup data, assuming either complete constructive or complete destructive interference.

at 95 Mev; the dotted curves are a result of this analysis at 146 Mev. In this curve are shown also the Hulthén wave function and the Gartenhaus wave function, normalized to fit the destructive interference curve, the most likely curve as previously observed, at $k=0.72$ fermi^{-1}. We observe a large momentum component larger than given by the repulsive core in the Gartenhaus wave function. Unfortunately the analysis has sufficient uncertainties that no firm conclusion may be drawn.

SUMMARY

The elastic p-d scattering at small angles may be quite well understood in terms of the theory of Kerman, McManus, and Thaler,[1] though the polarization does not fit too well in the Coulomb interference region.

The Chew-Goldberger[2] theory accounts qualitatively for the pickup peak in the elastic scattering near 180° cm. It is not yet possible to obtain definitive information about the deuteron wave function at large momenta although unusually large values are suggested.